Journal of Thermal Analysis and Calorimetry, Vol. 60 (2000) 377–390

DETERMINATION OF ACTIVATION ENERGY FOR GLASS TRANSITION OF AN EPOXY ADHESIVE USING DYNAMIC MECHANICAL ANALYSIS

G. Li[1], *P. Lee-Sullivan*[1*] *and R. W. Thring*[2]

[1]Department of Mechanical Engineering, University of New Brunswick
[2]Department of Chemical Engineering, University of New Brunswick, P. O. Box 4400 Fredericton N. B., E3B 5A3 Canada

(Received October 8, 1998; in revised form June 5, 1999)

Abstract

The activation energy associated with the glass transition relaxation of an epoxy system has been determined by using the three-point bending clamp provided in the recently introduced TA Instruments DMA 2980 dynamic mechanical analyzer. A mathematical expression showing the dependency of modulus measurements on the sample properties and test conditions has also been derived. The experimental results showed that the evaluation of activation energy is affected by the heating rate and test frequency, as well as the criterion by which the glass transition temperature (T_g) is established. It has been found that the activation energy based on the loss tangent (tanδ) peak is more reliable than on the loss modulus (E_2) peak, as long as the dynamic test conditions do not cause excessive thermal lags.

Keywords: activation energy, dynamic mechanical analysis (DMA), epoxy adhesive, glass transition

Introduction

Thermoset-based epoxy adhesives are extensively used to join engineering structures and to repair damaged components. For each type of epoxy adhesive, the final mechanical properties of the cured adhesive which affect bond strength and service life are very sensitive to the curing time and temperature. It is therefore, often necessary to conduct simple, short-term laboratory tests to evaluate the large number of epoxy resins available commercially in order to select the most appropriate adhesive. The glass transition temperature, T_g, which delimits the range of service temperature is considered a reliable indicator of completeness of cure and thus is used as a quality control tool. Traditionally, differential scanning calorimetry (DSC) is used to determine, for polymers, both reaction kinetics of curing and the respective thermal transitions such as T_g.

* Author to whom all correspondence should be addressed.

1418–2874/2000/ $ 5.00
Akadémiai Kiadó, Budapest

The dynamic mechanical analyzer (DMA) is a thermal analysis instrument which measures the viscoelastic response of materials either as a function of a linear heating rate, or as a function of time at a given temperature. The T_g can be measured with high sensitivity by monitoring the response of either the storage modulus (E_1), loss modulus (E_2), or loss tangent (tanδ) as a function of temperature [1, 2]. E_1 represents the elastic or fully recoverable energy during deformation while E_2 represents the viscous or net energy dissipated. Tanδ is the ratio of loss to storage modulus, which combines the viscous and elastic components into a single term and, thus, can summarize the curing behaviour of the polymer.

In dynamic mechanical analysis, T_g can either be defined as the temperature where the maximum loss tangent or the maximum loss modulus is observed, or as the inflexion point at which a significant drop of the storage modulus occurs. However, the respective peaks or points usually occur at different temperatures which results in a broad transition region for polymeric resins [1].

In addition to the inherent resin chemical properties and the used criterion of estimating the T_g value, factors related to instrument and test conditions, such as test frequency, heating rate, sample size and clamping effects can also influence the measured T_g value. It has been reported that increasing of the test frequency or heating rate leads to a shift of T_g to higher temperatures [1]. This implies a rather subjective evaluation of the degree of cure or cross-linking, and causes difficulty in assessing possible thermal and moisture effects.

The purpose of this investigation was to determine the influence of the DMA test frequency and heating rate on the evaluation of the activation energy related to the glass transition relaxation. As far as we know, there are only a few studies concerning the use of DMA methods for determining the activation energy of T_g [e.g. 3]. The study in reference [3], however, used only a single heating rate of 5°C min^{-1}.

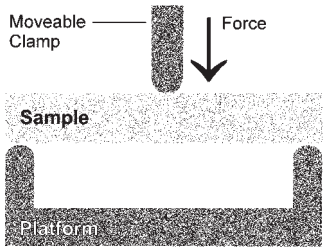

Fig. 1 Schematic presentation of three-point bending clamp used in the TA Instruments DMA 2980

Our study was conducted by using the newly commercialized TA 2980 DMA instrument. The TA Instruments DMA 2980 is a constant force oscillating DMA which was introduced in mid-1996 into the North American market. The machine offers a variety of clamping configurations ranging from single/dual-cantilever, three-point bend, tension/compression and shear sandwich modes. Preliminary investigations have been performed in our laboratory to determine the dependence of E_1 measure-

ments on the sample span-to-thickness ratio, drive amplitude, and clamping technique used [4]. The three-point bend mode, illustrated in Fig. 1, was studied in detail because the deformation is 'purer' than either of the single/dual cantilever or tension modes since clamping effects are eliminated [5]. It is also the only known deformation mode which has been designated as an ASTM Standard Test and is still subjected to review by an ASTM task group [6].

This paper will first present an expression derived from mechanics analysis to show how the material and test conditions such as material density, test angular frequency, phase lag, and specimen geometry can affect the material modulus. Results of T_g measurements for various heating rates and frequencies, and calculations of activation energies are then provided.

Principles of T_g measurements using DMA

The DMA detects the relaxation behaviour of a solid or viscoelastic liquid by applying a small oscillating force on the sample. When a sinusoidal stress is applied to a polymer sample, the strain lags behind the stress because of the viscoelastic response of the polymer. The strain and stress can be represented by [7]:

$$\varepsilon=\varepsilon_o \exp(i\omega t) \tag{1}$$

$$\sigma=\sigma_o \exp(i(\omega t+\delta)) \tag{2}$$

where ω is the angular frequency and δ the phase lag. The complex modulus is given by:

$$E^*=\frac{\sigma}{\varepsilon}=\frac{\sigma_o}{\varepsilon_o}(\cos\delta+i\sin\delta) \tag{3}$$

For the linear viscoelastic materials, the complex modulus would therefore have in-phase and out of phase $\pi/2$ components:

$$E^*=E_1+iE_2 \tag{4}$$

E^* is a complex dynamic mechanical tensile (or flexural) modulus where the real part $E_1=\sigma_o/\varepsilon_o\cos\delta$, is the in-phase storage modulus and the imaginary term $E_2=\sigma_o/\varepsilon_o\sin\delta$, is the out-of-phase loss modulus. E_1 is related to the mechanical energy stored per cycle and E_2 is related to energy dissipated or converted to heat through viscous flow. Tanδ is defined as the ratio of energy dissipated to energy stored per cycle of deformation, i.e.:

$$\tan\delta=\frac{E_2}{E_1} \tag{5}$$

Typically, it has been observed that the E_1 inflexion point occurs at the lower temperature, followed by the E_2 peak and finally by the tanδ peak [2]. However, in their explanation of how the tanδ peak is at a higher temperature than that of E_2, it is assumed by [2] that the point of inflexion in E_1 and the maximum in E_2 occurs at a temperature $T=T_o$. Therefore:

$$\frac{\mathrm{d}(\tan\delta)}{\mathrm{d}T}=\frac{\mathrm{d}}{\mathrm{d}T}\left(\frac{E_2}{E_1}\right)=\frac{\left(\frac{\mathrm{d}E_2}{\mathrm{d}T}\right)E_1-E_2\left(\frac{\mathrm{d}E_1}{\mathrm{d}T}\right)}{E_1^2}=\frac{-E_2\left(\frac{\mathrm{d}E_1}{\mathrm{d}T}\right)}{E_1^2} \tag{6}$$

and

$$\frac{\mathrm{d}E_2}{\mathrm{d}T}\Big|_{T=T_o}=0,\ \frac{\mathrm{d}E_1}{\mathrm{d}T}\Big|_{T=T_o}<0 \tag{7}$$

$$\therefore\frac{\mathrm{d}(\tan\delta)}{\mathrm{d}T}\Bigg|_{T=T_o}=\frac{-E_2\frac{\mathrm{d}E_1}{\mathrm{d}T}}{E_1^2}>0 \tag{8}$$

The above expressions show that tanδ curve is still rising at the peak temperature of E_2 and will subsequently reach a maximum at a temperature T_1(T_1>T_o). Mathematically, the peak arises as a ratio of the largest value of E_2 and the smallest value of E_1.

For highly cross-linked polymers, the T_g region is rather broad and depends on test parameters such as test frequency and heating rate. Because of the relatively broad T_g temperature range of thermosets, it would be inappropriate to choose the higher tanδ peak temperature as the T_g value, at which the polymer is already in a very soft rubbery state showing a very low storage modulus. In engineering applications, as the T_g is not a specific temperature, the T_g range extends from the inflexion point of the E_1 curve to the tanδ peak temperature. According to the ASTM D4065-94 [8], the recommended standard for reporting T_g is the temperature of the E_2 peak temperature. The tanδ peak temperature would exceed the softening point of the polymer, as explained in Eq. (8). It is proposed here that only if more conservative estimates are applied, the onset point temperature of storage modulus can be used.

Theoretical analysis of modulus measurements by three-point bending

In simple bending theory, any deflection due to the shear stress, τ, can be ignored for slender beams. However, when thick beams are used, considerable shear deflections are possible.

In the following, an expression is derived to calculate the material modulus as function of the measured material stiffness, phase lag, geometry, and test angular frequency, using a three-point bend dynamic test. We define the mid-span beam deflection by Δ, which is the sum of deflections of the bending moment [9–11]. By using the complex flexure modulus, E^*, to replace the tensile modulus, E, the following expressions are obtained:

$$\Delta=\Delta_b+\Delta_s \tag{9}$$

$$\Delta_b = \frac{PL^3 \sin\omega t}{48E^* I}$$
$$(\Delta_s)_1 = \frac{F_m}{2AG^*}\frac{L}{2} = \frac{F_m L(1+\nu)}{2AE^*} \quad (10)$$
$$(\Delta_s)_2 = \frac{F_m L(1+\nu/2)h^2}{16E^* I}$$

where Δ_b – the deflection due to bending, F_m – the measured reaction supporting and drive force, P – centrally applied dynamic load, L – beam span, ν – Poisson's ratio, G^* – complex shear modulus, ρ – material density, δ – measured phase lag, ω – angular frequency, A – sample cross-sectional area and I – area moment of inertia.

$\Delta_s=(\Delta_s)_i$, i=1, 2 are the simple and more precise solutions for mid-span beam deflections [9, 10], respectively, due to the shear force (neglecting the inertial force influence along the beam). For the rectangular cross section beam sample, $I=bh^3/12$ where b and h are sample width and thickness.

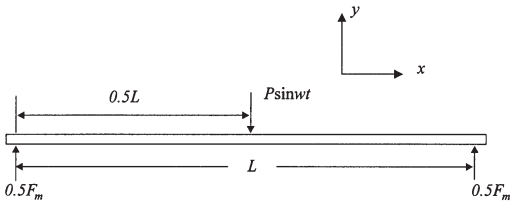

Fig. 2 Loading analysis of three-point bending

Assuming that the shape of the dynamic response of the beam is identical with the deflection of the beam subjected to a centrally concentrated load, $P\sin\omega t$ [11], Fig. 2, and that the bending deflections are symmetrical about the centre line, the deflection is thus given by:

$$y = \frac{P\sin\omega t}{48E^* I}(3L^2x - 4x^3),\ (0 \le x \le L/2) \quad (11)$$

The acceleration can then be formulated as:

$$\frac{d^2y}{dt^2} = -\frac{P\omega^2 \sin\omega t}{48E^* I}(3L^2x - 4x^3) \quad (12)$$

where the minus sign means the acceleration direction is opposite to the direction of the applied force, $P\sin\omega t$. By integrating, the inertial force is given by:

$$m\frac{d^2y}{dt^2} = -\frac{5PL^4\omega^2\rho A\sin\omega t}{384E^* I} \quad (13)$$

Using Newton's second law, as in [12], we obtain:

$$F_m = P\sin\omega t + \frac{5PL^4\omega^2\rho A}{384E^*I}\sin\omega t \tag{14}$$

The second term in Eq. (14), which is due to inertial effects, is very small. Thus the deflection generated by the shear force, $0.5F_m \approx 0.5P\sin\omega t$, can be written as:

$$\begin{aligned}(\Delta s)_1 &= \frac{PL(1+\nu)}{2AE^*}\sin\omega t \\ (\Delta s)_2 &= \frac{PL(1+\nu/2)h^2}{16E^*I}\sin\omega t\end{aligned} \tag{15}$$

The simple solution for the complex modulus, E^*, can be found by dividing Eq. (14) by $\Delta=\Delta_b+(\Delta_s)_1$ to give:

$$\begin{aligned}K_m e^{i\delta} &= \frac{F_m}{\Delta} = \frac{E^*}{\frac{L^3}{48I}+\frac{(1+\nu)L}{2A}}\left(1+\frac{5L^4\omega^2\rho A}{384E^*I}\right) \\ \Rightarrow E^* &= K_m e^{i\delta}\left(\frac{L^3}{48I}+\frac{(1+\nu)L}{2A}\right)-\frac{5L^4\omega^2\rho A}{384I}\end{aligned} \tag{16}$$

where K_m is the measured material stiffness.

Accordingly, a more precise solution for a rectangular cross-sectional beam can be found using $\Delta=\Delta_b+(\Delta_s)_2$ to give:

$$\begin{aligned}K_m e^{i\delta} &= \frac{F_m}{\Delta} = \frac{E^*}{\frac{L^3}{48I}+\frac{(1+\nu/2)Lh^2}{16I}}\left(1+\frac{5L^4\omega^2\rho A}{384E^*I}\right) \\ \Rightarrow E^* &= K_m e^{i\delta}\left(\frac{L^3}{48I}+\frac{3(1+\nu/2)L}{4A}\right)-\frac{5L^4\omega^2\rho A}{384I}\end{aligned} \tag{17}$$

The storage modulus and loss modulus, respectively, are given by the real and imaginary parts of the above equations. If the influence of shear terms are neglected, Eq. (17) becomes identical with Eq. (16), and is very close to the result obtained in reference [12]. Moreover, if the frequency term is neglected, as would be in quasi-static tests such as creep or stress relaxation, Eq. (17) is very similar to the expression given in the TA 2980 DMA technical manual [13].

Determination of activation energy using Arrhenius relationship

The activation energy of the glass transition, ΔH, can be obtained by applying the Arrhenius law [7]. In dynamic mechanical experiments, ΔH can be estimated by using the time-temperature superposition principle, to superimpose the tanδ peaks determined at different test frequencies [3]. Accordingly, individual tanδ peaks can be

shifted for superposition along the logarithmic time axis by the shift factor, $\log a_T$. The temperature dependence of the test frequency may then be expressed as [7]:

$$f = f_o \exp\left(-\frac{\Delta H}{RT}\right) \tag{18}$$

where f and f_o are analogous to the rate constant and pre-exponential factor of the Arrhenius equation and R is the gas constant. The shift of the glass transition temperatures, T_{g1} and T_{g2}, due to change in the test frequencies f_1 and f_2 allows the determination of the activation energy of T_g [7]:

$$\frac{f_1}{f_2} = \frac{\exp(-\Delta H/RT_{g1})}{\exp(-\Delta H/RT_{g2})} \tag{19}$$

$$\log\left(\frac{f_1}{f_2}\right) = \log a_T = \frac{\Delta H}{R}\left(\frac{1}{T_{g2}} - \frac{1}{T_{g1}}\right)\log e \tag{20}$$

$$\Delta H = -R\left[\frac{\mathrm{d}(\ln f)}{\mathrm{d}(1/T_g)}\right] \tag{21}$$

Equation (21) describes the temperature-dependence of polymer relaxations, where ΔH is the activation enthalpy of the glass transition relaxation. In [3] this approach was applied for determining ΔH, although the authors plotted the $\log f$ rather than $\ln f$ and only used a single heating rate of 5°C min^{-1}.

Experimental

Materials

An epoxy novolac resin, EP45HT, manufactured by Master Bond Inc. was tested. Novolac resins are characterized by a better elevated-temperature performance than the bisphenol-A based resins. EP45HT was mixed 100 parts mass of the epoxy to

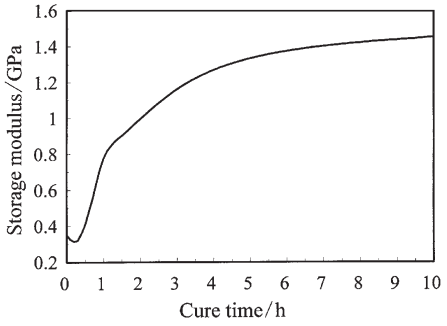

Fig. 3 The variation of storage modulus with cure time for EP45HT epoxy resin

Table 1 DMA results of average T_g based on three criteria

Frequency, *f*/Hz	Heating rate/ °C min^{-1}	E_1, inflexion point temperature/°C			E_2 peak temperature/°C			tanδ peak temperature/°C		
		S1	S2	Avg.	S1	S2	Avg.	S1	S2	Avg.
1	1	120.29	118.95	119.62	128.08	127.72	127.90	138.10	138.45	138.28
	2	120.94	122.08	121.51	129.38	128.97	129.18	139.84	140.23	140.04
	3	123.35	124.97	124.16	130.32	131.53	130.93	141.99	142.39	142.19
	5	127.94	127.57	127.76	138.77	137.16	137.97	147.22	147.22	147.22
5	1	123.22	124.57	123.90	130.23	129.92	130.08	143.10	142.80	142.95
	2	121.78	123.51	122.65	130.72	129.15	129.94	144.81	144.89	144.85
	3	125.75	124.74	125.25	132.35	132.74	132.55	146.54	146.42	146.48
	5	130.77	131.30	131.04	138.37	136.36	137.37	150.44	151.25	150.85
10	1	120.52	120.97	120.75	130.58	130.32	130.45	144.89	144.81	144.85
	2	123.62	126.04	124.83	129.52	129.92	129.72	146.42	146.82	146.62
	3	128.44	128.40	128.42	132.74	131.13	131.94	148.43	148.83	148.63
	5	134.47	131.27	132.87	139.18	139.18	139.18	154.06	153.66	153.86
30	1	122.28	121.40	121.84	132.37	130.58	131.48	148.83	147.75	148.29
	2	127.10	125.98	126.54	131.53	129.92	130.73	150.85	149.24	150.05
	3	128.73	130.94	129.84	130.72	133.14	131.94	152.05	152.05	152.05
	5	133.25	135.78	134.52	139.18	139.58	139.38	156.48	157.28	156.00

30 parts mass of an aromatic amine blend [13]. The epoxy resin was supplied with a recommended range for curing time and temperature. There is no specification for the minimum curing time for a particular curing temperature. It was therefore necessary to determine an appropriate curing time. The test was conducted by using an 8 mm span dual-cantilever clamp under isothermal conditions at 121°C. The samples were prepared by applying a thin layer of liquid resin onto a cotton strip of 30 mm length× 10 mm width which was then wrapped with thin aluminum foil. The curing time dependence of E_1 for the studied epoxy is shown in Fig. 3. The gel point may be identified by an initial small peak on the shoulder of the curing curve. Based on the time needed to reach a stationary E_1 value, it can be estimated that the epoxy should be cured for at least 10 h to reach the maximum curing level.

Determination of glass transition range

A second batch of liquid resin was cast in a 140×140 mm glass mould and cured at 121°C for 12 h. DMA samples of size 25×10×3 mm were cut from the cast epoxy block and tested using the 20 mm span three-point bend clamp at linear heating rates 1, 2, 3 and 5°C min^{-1}. A test frequency of 1, 5, 10 and 30 Hz was applied for each heating rate. The T_g range was determined during scanning from room temperature (*RT*) to 200°C. Each test was repeated using new samples cut from the same cast block.

Results and discussion

Figure 4 shows a typical plot of the temperature dependence of E_1, E_2 and tanδ. Table 1 presents the results for the evaluated T_g values based on the three criteria. Since the average values for E_1 are the lowest, only the results for E_2 and tanδ have been plotted. It can be seen in Fig. 5 that by increasing the heating rate shifts T_g to higher temperatures. This is consistent with the results of reference [1]. It is also evident that the E_2 peaks are less influenced by the test frequency. If, however, the tanδ criteria is used, T_g increases directly with the test frequency for a constant heating rate.

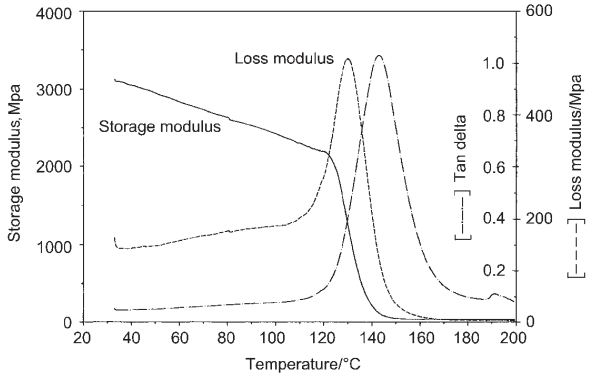

Fig. 4 Superposition of typical plots showing the variation of E_1, E_2 and tanδ with increasing temperature. Sample: EP45HT, size: 20.0×9.75×2.59 mm

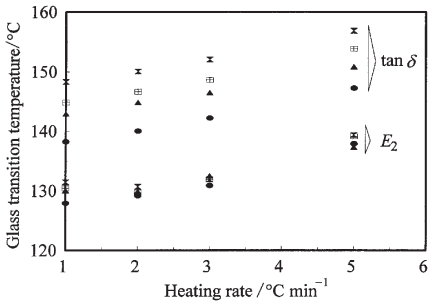

Fig. 5 Glass transition temperatures based on the E_2 and tanδ peaks. • – 1 Hz, ▲ – 5 Hz, ⊠ – 10 Hz, x – 30 Hz

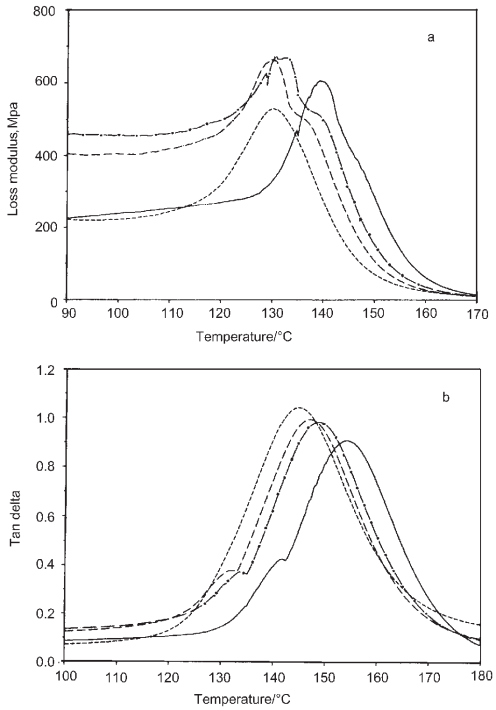

Fig. 6 The effects of increasing heating rate on the T_g value based on a – E_2 peak and b – tanδ peak. Test frequency=10 Hz. — 1°C min^{-1}, --- 2°C min^{-1}, ·-·-· 3°C min^{-1}, ▬ 5°C min^{-1}

Figures 6 and 7 show the direct effects of increasing heating rate and test frequency on the glass transition temperatures. As expected, increasing heating rate and test frequency results in an increase of T_g. In Fig. 6(a), a double T_g artifact can be observed in the E_2 plots when the heating rate is between 2–3°C min^{-1}. The second

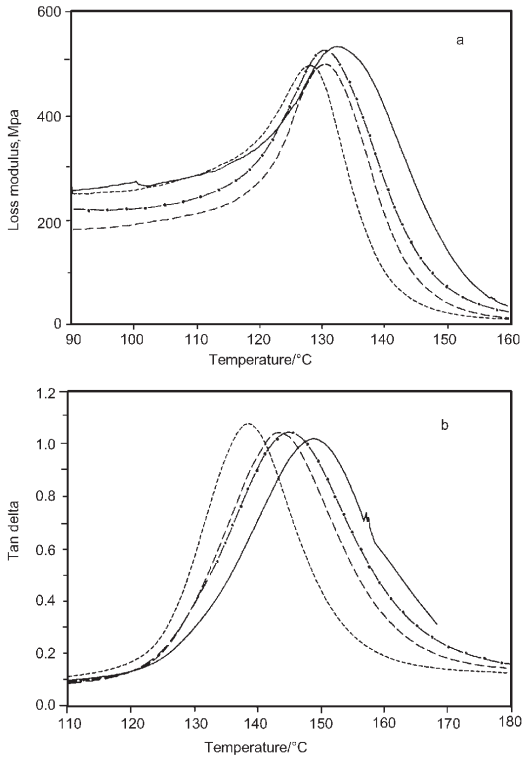

Fig. 7 The effects of increasing test frequency on the T_g value based on a – E_2 peak and b – tanδ peak. Heating rate=1°C min^{-1}, ···· 1 Hz, --- 5 Hz, ·-·-· 10 Hz, ——30 Hz

peak, however, does not appear in the tanδ plots even though it was reported in reference [1] and attributed to the thermal lag at the clamped regions in their instrument. In our DMA instrument, however, we observed small peaks at the shoulder of the curves at the higher heating rates, Fig. 6. There are, however, no visible artifacts in either the E_2 or the tanδ curves when the test frequency is varied (Fig. 7).

For the 1–5°C min^{-1} and 1–30 Hz ranges, the mean T_g was observed to be between 128–139°C based on E_2 peaks and between 138–156°C using tanδ peaks. Generally, there is a greater scatter at higher heating rates and frequencies. This is because it is more difficult to achieve thermal uniformity across the entire sample at higher heating rates and frequencies since the segmental molecular motions and molecular relaxations lag behind the temperature change. The thermal lag delays the onset of glass transition. Since the sample thermocouple is not in direct contact with the sample, the time to reach thermal equilibrium will inherently depend upon the mass of the specimen, the thermal conductivity, and the gripping arrangement [1, 8].

Table 2 shows the values of ln$f$ and $(1/T_g)$ for T_g determined from the tanδ and E_2 peaks. They are plotted as $(1/T_g)$ *vs*. ln$f$ in Figs 8 and 9, respectively. The curves are linear between 1–10 Hz but become non-linear at 30 Hz. According to Eq. (21), the

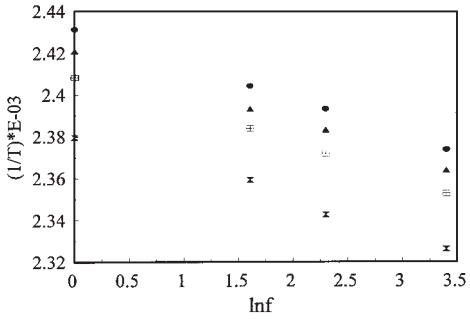

Fig. 8 Plot of $(1/T_g)$ *vs.* ln*f* based on tanδ peaks. • – 1°C min^{-1}, ▲ – 2°C min^{-1}, ▫ – 3°C min^{-1}, x – 5°C min^{-1}

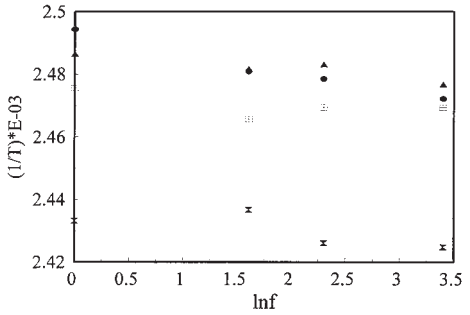

Fig. 9 Plot of $(1/T_g)$ *vs.* ln*f* based on E_2 peaks. • – 1°C min^{-1}, ▲ – 2°C min^{-1}, ▫ – 3°C min^{-1}, x – 5°C min^{-1}

activation energy related to the glass transition is obtained by multiplying the slopes of the $1/T$ *vs.* ln*f* plot with the gas constant, R=8.314·10^{-3} kJ mol^{-1} K^{-1}. Since T_g will depend on the selection criterion, the slopes would therefore be different for tanδ ($T_{tan\delta}$) and E_2 (T_{E2}) peaks.

Table 2 Values of ln*f* and $(1/T_g)$ based on tanδ and E_2 peaks

Frequency, *f*/Hz	ln*f*	@ 1°C min^{-1}		@ 2°C min^{-1}		@ 3°C min^{-1}		@ 5°C min^{-1}	
		$1/T_{tan\delta}$	$1/T_{E2}$	$1/T_{tan\delta}$	$1/T_{E2}$	$1/T_{tan\delta}$	$1/T_{E2}$	$1/T_{tan\delta}$	$1/T_{E2}$
		10^{-3} K^{-1}		10^{-3} K^{-1}		10^{-3} K^{-1}		10^{-3} K^{-1}	
1	0	2.431	2.494	2.421	2.487	2.409	2.476	2.38	2.433
5	1.61	2.404	2.481	2.393	2.482	2.384	2.466	2.359	2.437
10	2.3	2.393	2.479	2.383	2.483	2.372	2.470	2.343	2.426
30	3.4	2.373	2.472	2.364	2.477	2.353	2.470	2.326	2.425

Assuming that the highest heating rate for 30 Hz would lead to excessive thermal lags, the activation energies, ΔH, for the various heating rates were calculated first for the 1–10 range and then for the entire 1–30 Hz range, using linear regression analysis (Table 3). The correlation coefficients, (R^2), have also been included. It is evident that ΔH calculated from the $T_{tan\delta}$ criterion is more consistent than T_{E2}. More-

over, the activation energies increase with heating rate. The trend is clear for $\Delta H_{tan\delta}$ but there is too much scatter for the ΔH_{E2}.

Table 3 Activation energies ΔH calculated from tanδ and E_2 peaks and correlation coefficient (R^2)

Freqency, f/Hz	Heating rate/ °C min^{-1}	Calculated activation energies			
		$(\Delta H)_{tan\delta}$/kJ mol^{-1}	R^2	$(\Delta H)_{E2}$/kJ mol^{-1}	R^2
1, 5, 10	1	498.90	0.9997	1168.31	0.973
	2	499.88	0.999	4847.53	0.697
	3	524.31	0.999	2526.77	0.60555
	5	537.27	0.972	3835.47	0.221
1, 5, 10, 30	1	491.42	0.9997	1289.91	0.976
	2	496.30	0.999	3252.06	0.846
	3	506.60	0.999	4833.36	0.357
	5	520.82	0.987	2933.92	0.502

It has been proposed that the maximum heating rate in DMA tests should not exceed 2°C min^{-1} [1]. If only the 1–2°C min^{-1} range is considered, the average $\Delta H_{tan\delta}$ for the glass transition of this epoxy system can be estimated as 499 kJ mol^{-1}. The obtained results confirm that the Arrhenius relationship shown in Eq. (21) is valid only for heating rates less than 2°C min^{-1}, where a consistent value for the activation energy can be obtained. At heating rates within this range, the shift factor (α_T) is only related to the test frequency, in accordance to the Arrhenius relationship, and not dependent on the heating rate itself. At higher heating rates, thermal and material diffusion become dominant factors causing increasingly higher activation energies [14].

Conclusions

Based on experiments conducted on an epoxy adhesive using the TA Instruments 2980 dynamic mechanical analyzer, the following conclusions can be made:

1. The T_g value for epoxy resins based on the tanδ peak is significantly influenced by the test frequency. T_g, on the other hand, is more consistent if the value is based on the loss modulus peak. Irrespective of the criteria used, however, T_g is shifted to higher temperatures when testing is performed at high heating rates.

2. Activation energies for the glass transition relaxation determined from loss tangent (tanδ) peaks are more reliable than using the loss modulus (E_2) criterion. In the former method, the activation energy remains consistent for a 1–2°C min^{-1} heating rate and 1–10 test frequency range, where the relaxation appears to follow the first order kinetics Arrhenius relation. The activation energy, however, tends to increase slightly at higher heating rates and frequencies. For E_2 criterion, there is too much scatter to estimate the activation energy with any confidence.

References

1 R. Chartoff, P. T. Weissman and A. Sircar, Assignment of the Glass Transition, ASTM STP 1249, R. J. Seyler, Ed., ASTM, PA, 1994, p. 88.
2 M. Akay, Composites Sci. and Tech., 47 (1993) 419.
3 L. Barral, J. Thermal Anal., 41 (1994) 1463.
4 P. Lee-Sullivan and D. Dykeman, Amplitude Effects, Polymer Testing, Vol. 19, No. 2 (2000) p. 115.
5 S. Qing and P. Lee-Sullivan, Polymer Testing, Vol. 19, No. 3 (2000) p. 237.
6 Standard Test Method for Measuring the Dynamic Mechanical Properties of Plastics using Three-Point Bending, ASTM D5023-94, ASTM, PA.
7 I. M. Ward and D. W. Hadley, An Introduction to the Mechanical Properties of Solid Polymers, Wiley, New York 1993.
8 Standard Practice for Determining and Reporting Dynamic Mechanical Properties of Plastics, ASTM D4065-94, ASTM, PA.
9 J. G. Williams, Stress Analysis of Polymers, Wiley, New York 1973.
10 F. P. Beer and E. R. Johnston, Mechanics of Materials, Metric Edition, McGraw-Hill, 1992.
11 J. L. Humar, Dynamics of Structures, Prentice-Hall, USA 1990.
12 R. Greif and M. S. Johnston, J. Eng. Mater. and Tech., 114 (1992) 77.
13 Technical Data Sheet, MasterBond Polymer System EP45HT, MasterBond Inc.
14 J. H. Flynn, J. Thermal Anal., 36 (1990) 1579.